

Theory of electric corona including the role of plasma chemistry

J. J. Lowke and R. Morrow.

CSIRO Division of Applied Physics, Sydney, Australia, 2070.

Abstract: The traditional theory of corona is cast in terms of ionization and attachment coefficients and gives good quantitative predictions of the voltage for the onset of corona as a function of the diameter of the corona wires, temperature, pressure and characteristics of the gas. Furthermore, it gives a fair qualitative description of the corona discharge itself as a function of space and time. The motion of electrons, positive ions and negative ions formed by electron attachment, can produce distortions to the electric field by space charge effects which result in Trichel current pulses for negative voltages and "streamers" for positive voltages. Recently it has been realized that the medium of the corona discharge in air, for example, is not ordinary air, since the properties of the air are changed by the corona discharge itself. Of particular importance for properties of the corona discharge are the many excited states and metastable atoms and molecules that are created by the corona discharge, which may influence the electron density by detachment of negative ions or make possible two-step ionization. Rate constants of those reactions of plasma chemistry, which involve electrons in the discharge, are a function of the local electric field. In the present paper, mechanisms of plasma chemistry are proposed to explain the voltage for spark breakdown between corona wires.

INTRODUCTION

Electric corona has important industrial applications such as in electrostatic precipitators, the commercial production of ozone in "corona" barrier discharges for disinfectant purposes and for the treatment of surfaces, for example those of paper used in photocopiers. Recently much interest has been aroused by the discovery that corona produced using pulsed voltages applied to electrostatic precipitators can markedly reduce the concentrations of NO_x and SO_x concentrations in flue gases, provided that the pulse rise times are less than a microsecond (1). The recent increase in interest in environmental issues has led to renewed interest in basic aspects of corona. With a better theoretical understanding of corona we might be able to answer such questions as (a) why is it necessary for coronavoltages to be pulsed to remove NO_x and SO_x , and (b) whether is it possible to build more efficient ozonizers without them being poisoned by the production of oxides of nitrogen.

The theory of corona divides itself naturally into three distinct subjects. (1) Corona onset voltages can be predicted for air by application of the Townsend replacement criterion to the region adjacent to the corona wire, where the electrostatic field is so high that the ionization coefficient is higher than the attachment coefficient. (2) The qualitative characteristics of Trichel pulse corona, including discharge characteristics and charge densities as a function of space and time, have also been derived using ionization and attachment coefficients. (3) Experimental observations of spark breakdown between precipitator wires show the spark breakdown voltage to be almost independent of wire diameter and also to increase almost linearly with wire separation. These remarkable results have not been previously explained theoretically, but in the present paper it is proposed that they are explicable in terms of plasma chemistry. Plasma reactions of the gas involving metastables and excited states can influence electron attachment and detachment and can change the electric field for a given current density by a factor of six.

VOLTAGE FOR CORONA ONSET.

An important quantity for the design of equipment involving the production of corona by the application of a high voltage to wires is the voltage at which the corona discharge is initiated. Peek (2) measured corona onset voltages as a function of wire radius, wire material, gas temperature and gas pressure and obtained the following formula entirely by empirical means for the corona onset field, E , at the wire surface:

$$E = 30 \delta [1 + 0.3 / (a \delta)]^{1/2} \tag{1}$$

where a is the wire radius and $\delta = N/N_0$, the relative number density of the gas. Thus the value of δ accounts for variations with temperature T and pressure p , using the gas law $p = N k T$, where N is the gas number density, k is Boltzmann's constant and N_0 is the number density at normal temperature and pressure.

Central to any theoretical explanations of corona are ionization and attachment. At high electric fields electrons are accelerated to such an extent that they ionize the gas, producing new electrons. However, electrons can attach to molecules to form negative ions, particularly at low energies. It is in attaching gases such as air, oxygen and sulphur hexafluoride that corona occurs. Ionization and attachment rates are represented by α and η , which are respectively the number of ionizing and attachment processes undergone by each electron per cm of drift in the electric field. The quantities α/N and η/N can be measured directly, or calculated from measurements of basic cross sections for ionization and attachment, which are functions of electron energy. The calculations also require the determination of the electron energy distribution function through a solution of the Boltzmann equation for each value of E/N . Such calculations of ionization and attachment coefficients are consistent with experiments, at least for the common gases such as oxygen, nitrogen, carbon dioxide, water vapor and sulphur hexafluoride, and also for mixtures of gases such as air. In Fig. 1 are shown calculated values of α/N and η/N as a function of E/N for air (3); m/N is defined later.

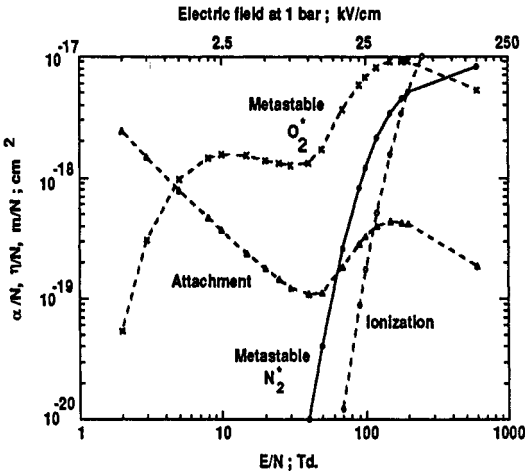


Fig.1 Calculated Coefficients for Air.

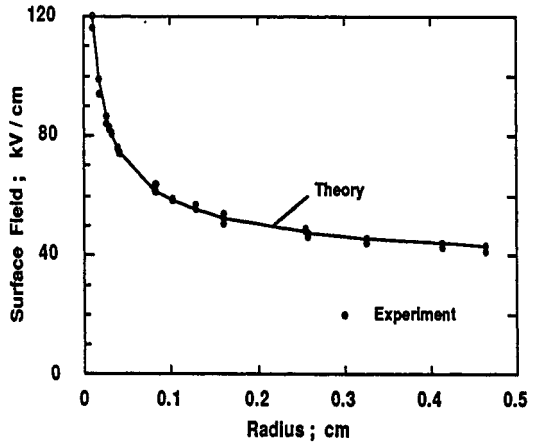


Fig. 2 Corona Onset Field for Wires.

From Fig. 1, note that there is a critical value of E/N of $E_0/N_0 \sim 120$ Td below which the attachment coefficient is greater than the ionization coefficient; $1 \text{ Td} = 10^{-17} \text{ V cm}^2$. When a voltage is applied to a wire, the field distribution around the wire, from a solution of Poisson's equation, $\nabla \cdot E = 0$, is $E \sim 1/r$. We choose the constant of proportionality to be such that $E = E_0 c \delta / r$, so that $r = c$ is the critical radius beyond which the values of E/N will be less than 120 Td and electrons will be converted to negative ions by attachment. However, for a corona discharge to exist, it is not sufficient for there to be a region near the wire for which $E/N > 120$ Td. The distance over which $E/N > 120$ Td must be such that the Townsend replacement criterion is fulfilled (4). This criterion states that in travelling across the ionization region, any electron starting at the cathode must be replaced at the cathode by processes from the discharge. Expressed mathematically, this criterion is

$$\gamma \exp(\int \alpha' dr) = 1, \tag{2}$$

where $\alpha' = \alpha - \eta$ is the net ionization coefficient and γ is the generalized secondary coefficient. The exponential gives the total number of electrons produced in the ionizing region by an electron; γ is the fraction of ionizing events that produces an electron at the cathode, e.g. by photo-emission, positive ion or metastable bombardment, or even photoionization. The integration in the exponential is taken from the surface of the wire at $r=a$ to $r=c$, beyond which there is no net ionization.

Peek's equation (1) can be derived from equ. (2) by approximating the net ionization coefficient as a linear function of E/N for the region near the critical $E/N = E_0/N_0$. Thus $\alpha'/N = A (E/N - E_0/N_0)$ where A can be obtained from Fig. 1. On substituting for α' in equ.(2), using $E = E_0 c \delta / r$, integrating from a to c , and using the approximation $\ln(1+x) = x - x^2/2$ where $x = (c-a)/a$, we obtain a value for c/a and thus an expression for E at $r=a$ of

$$E = E_0 \delta \{ 1 + [2 \ln(1/\gamma) / A E_0 \delta a]^{1/2} \}. \quad (3)$$

Equ. (3) is Peek's equation except that the empirical constants are in terms of constants having physical significance. The value of E_0 is the field for which ionization equals attachment at atmospheric pressure, which from Fig.1 for air is 30 kV/cm.

The value of $\ln(1/\gamma) / A$ for equ.(3) can be derived from the experimental results of the breakdown voltage as a function of the separation of plane electrodes, known as the Paschen curve (5). If our linearization for α'/N is again applied to Townsend's breakdown criterion, equ.(2), but for plane parallel geometry, we obtain an expression for the breakdown voltage between plane parallel plates of

$$V = E_0 \delta d + \ln(1/\gamma) / A. \quad (4)$$

From the experimental Paschen curve for air, over the range of a few mm for the plate separation d , $\ln(1/\gamma) / A = 1350$ (6). Equation (3) then becomes identical with equ (1). Despite the approximations made in the derivation of equ.(3), predictions of corona onset from the equation are in fair agreement with experimental values for wire radii ranging from 0.2 mm to 5 mm, temperatures from -10 C to 140 C and pressures from 0.05 to 1 bar. A comparison of experimental results from Peek (1) and the predictions from equ. (3) are shown in Fig. 2. The voltage for the onset of corona is obtained by integration of the electrostatic field for the particular geometry. For a wire-plate separation S , the voltage is given by

$$V = E_0 \delta \{ 1 + [2 \ln(1/\gamma) / A E_0 \delta a]^{1/2} \} a \ln(S/a). \quad (5)$$

CORONA THEORY INVOLVING IONIZATION AND ATTACHMENT COEFFICIENTS.

Corona discharge phenomena for voltages above the corona threshold voltage are complex (7,8,9). For voltages immediately above the threshold voltage, discharges are intermittent and generally irregular, as is the case for corona discharges in sulphur hexafluoride. However, for negative voltages applied to a point in air, very regular current pulses can be obtained, as discovered by Trichel (10). At higher voltages a glow discharge regime is obtained for both positive and negative corona. At still higher voltages there is spark breakdown to an arc. There are fairly striking differences between positive and negative coronas in air. Discharges in the Trichel pulse regime for negative corona have a visible region very close to the point, except for a dark space immediately next to the point. The frequency of the current pulses is closely proportional to the current. On the other hand, when similar positive voltages are applied to a point, the discharge is characterized by intermittent "streamers" or filamentary discharges, which extend a much greater distance from the point into the gap than for negative corona. Furthermore, there is no proportionality of the frequency of the discharges to current; instead the magnitude of each current pulse increases with total current.

The development of theoretical methods to make quantitative predictions of these discharge properties, or of the extent of the discharge modes, is beset with a number of problems. (a) Corona properties are basically two-dimensional, depending on both axial parameters and radial parameters such as the radius of the electrode point or wire. (b) Space charge effects involve the solution of Poisson's equation in which the difference between densities of positive and negative particles needs to be evaluated. For large number densities, numerical difficulties arise, as these densities then need to be determined very accurately. (c) Properties of cathode-directed streamers depend critically on photoionization coefficients, which determine the production rate of new electrons to enable streamers to travel against the electric field. The physical mechanism of such

photoionization is not at all clear, nor is it clear how to accurately represent these effects. (d) Corona effects involve time variations on a nanosecond time scale and also involve very large gradients in the electric field. Thus it is not clear that the electrons will be in equilibrium with the local electric field, which is a required condition for the transport coefficients of ionization, attachment and mobility to be valid.

Nevertheless, conventional transport theory has been used to make semi-quantitative predictions of Trichel pulses of negative corona in oxygen (11) and positive corona in sulphur hexafluoride (12,13). An assumption is made that the radius of the channel is constant, eg 0.1mm, and then space charge effects are calculated using the method of (14), so that the problem is reduced to a one-dimensional calculation. Problems in calculating convective transport to achieve the numerical accuracy that is necessary to account for space charge effects, can be overcome by using the method of flux-corrected transport (15). The numerical calculations employ a non-uniform mesh, which is moved to ensure that details of the high gradient region at the head of the streamer channel are retained.

The coupled equations for the conservation of electron, negative ion and positive ion densities are solved together with Poisson's equation. This solution gives the distribution of particle densities and electric field as a function of position and time. Thus a prediction is made of total current as a function of time. The electron continuity equation is

$$\partial n_e / \partial t = n_e \alpha w_e - n_e \eta w_e - \gamma_R n_e n_+ - \partial (n_e w_e) / \partial x; \tag{6}$$

n_e is the electron density, t is time, w_e is the absolute value of the electron drift velocity, γ_R is the electron ion recombination coefficient and x is the distance from the cathode. The term in α takes into account the production of electrons by ionization due to the electric field, the term in η accounts for the loss of electrons by attachment to oxygen to form negative ions, the term in γ accounts for the loss of electrons by recombination with positive ions and the term in x accounts for the flow of electrons due to the electric field. Similarly, the continuity equations for positive and negative ion densities, n_+ and n_- , are

$$\partial n_+ / \partial t = n_e \alpha w_e - \gamma_R n_e n_+ - \gamma_R n_- n_+ - \partial (n_+ w_+) / \partial x; \tag{7}$$

$$\partial n_- / \partial t = n_e \eta w_e - \gamma_R n_- n_+ - \partial (n_- w_-) / \partial x; \tag{8}$$

ion-ion recombination rates are taken to be the same as the electron-ion recombination rate. Account is taken of the modification to the imposed electrostatic electric field by space charge effects using the solution of Poisson's equation which is

$$\nabla \cdot E = e (n_+ - n_e - n_-) / \epsilon_0; \tag{9}$$

e is the electronic charge and ϵ_0 is the permittivity of free space.

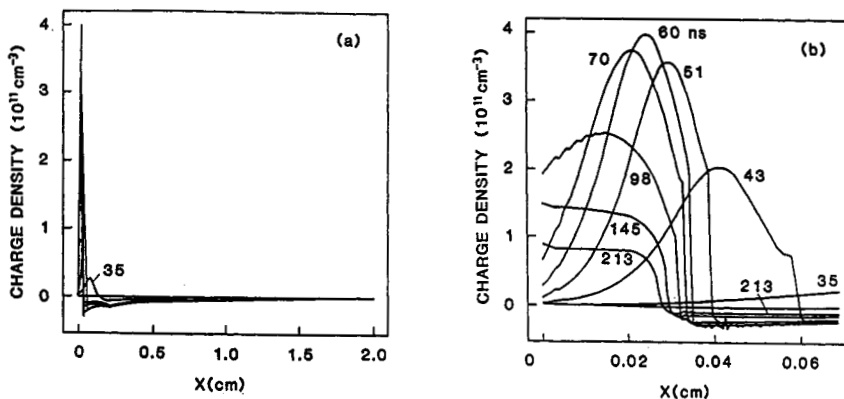


Fig. 3. Calculated Net Charge for Negative Corona in Oxygen; times marked in ns.

In Figs 3 - 5 are shown the calculated characteristics of the first Trichel pulse when a negative voltage of 2900 V is applied to a sphere of 0.5 cm radius located 2 cm from a plane in oxygen at a pressure of 50 Torr (11). Numerical results are in fair qualitative agreement with experimental results. The active region of the discharge only extends ~ 2 mm into the gap, and there is a dark space immediately in front of the cathode of

thickness ~ 0.2 mm. Electrons in the initial high field region near the sphere produce an initial rapidly increasing current with no space charge effects for the first part of the current pulse of Fig. 5, marked AB. But for later times a net positive charge accumulates in front of the cathode because of electrons moving away from the cathode. For distances of greater than ~ 0.3 mm there is a net negative charge due to the preponderance of negative ions. The effect of these charges is to reduce the high imposed electrostatic field near the point, see Fig.4. For times of greater than 50 ns the electric field is everywhere reduced to below the critical field for which ionization equals attachment, shown by E^* in Fig. 4. The very high electric field in the immediate vicinity of the cathode in Fig. 4 is over such a short distance that negligible contribution is made to the integral of equ. (2) for the Townsend replacement criterion. In the region CD of Fig. 5, the current falls primarily due to space charge effects reducing the field. For the region DE the current falls primarily due to electron attachment reducing the number of electrons. For the region EF, ion current is a significant fraction of the total current. When the number of ions is sufficiently reduced in the discharge gap so that the initial applied electrostatic field is restored, electrons emitted from the cathode, for example by the impact of metastables, will initiate another current pulse.

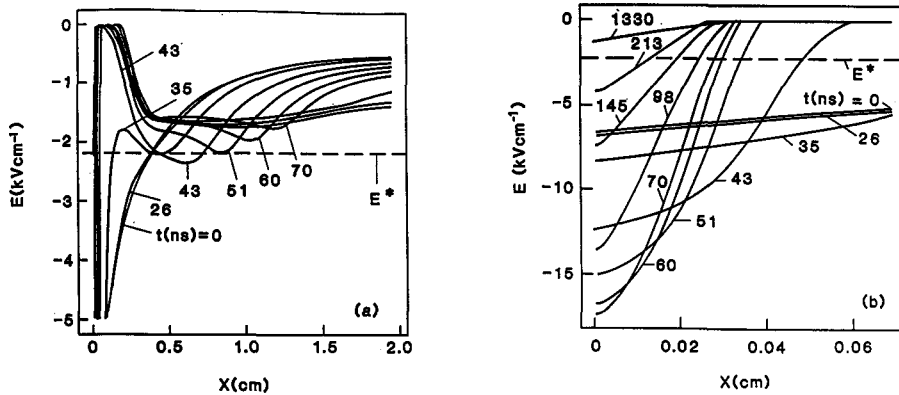


Fig. 4 Calculated Electric Field for Negative Corona in Oxygen.

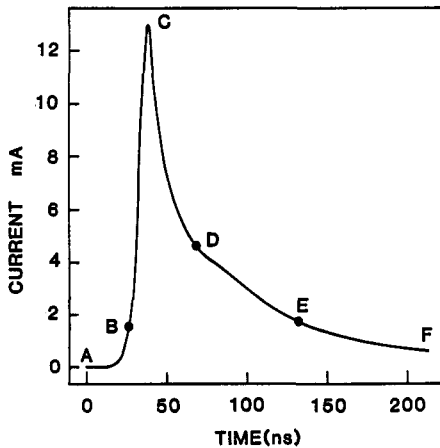


Fig. 5 Calculated Trichel Pulse Current in Oxygen.

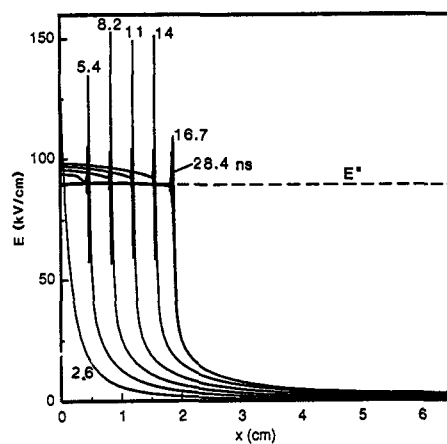


Fig. 6 Calculated Electric Field for Streamer in SF₆.

In Fig 6 is shown the calculated electric field for positive corona resulting from a voltage that is linearly rising to a maximum of 200 kV in 15 ns applied to a sphere of 2.5 mm radius located 6.5 cm from a plane in sulphur hexafluoride at atmospheric pressure. Sulphur hexafluoride is a very strongly attaching gas. The attachment time constant τ , is defined from $1/\tau = (1/n_e) \partial n_e / \partial t = -\eta w_e$. At the critical field E^* , τ is 0.1 ns for sulphur hexafluoride; for air, τ is 10 ns. For sulphur hexafluoride, $E^* = 90$ kV/cm; for air $E^* = 30$ kV/cm. The curves of Fig. 6 show the dominant role of electron attachment. Within the plasma, the electric field is closely given by E^* . The plasma front advances with the voltage as it is being applied and the length of the streamer is closely given by V/E^* at any given instant. Space charge effects adjust themselves

to maintain E within the plasma at the critical value. After the voltage attains its maximum value, the plasma and the arc current rapidly decay due to electron attachment. In Fig. 4 for oxygen, it is seen that space charge also tends to make the field within the plasma uniform at E^* , but the effect is much weaker.

SPARK BREAKDOWN

The limiting voltage for corona operation is the voltage for spark breakdown. This voltage is of significant practical importance as corona phenomena such as electrostatic precipitation and the destruction of NO_x and SO_x work better at higher voltages. In Fig. 7 are shown experimental measurements for air at atmospheric pressure taken by Peek (2), of the spark breakdown voltage between wires as a function of the distance between the wires and also for different wire diameters. The results of Fig. 7 are remarkable in that the breakdown voltage is largely independent of wire diameter and increases fairly linearly as the distance between the wires is increased. It is as if the corona discharge plasma has a given resistance per unit length, so that for increased length there is a corresponding linear increase in spark breakdown voltage. However, the characteristic field, obtained from Fig. 7 by dividing the voltage by the wire separation is $\sim 5 \text{ kV/cm}$, corresponding to $E^*/6$. It is as if the plasma chemistry of the corona discharge reduces the impedance of normal air by a factor of 6.

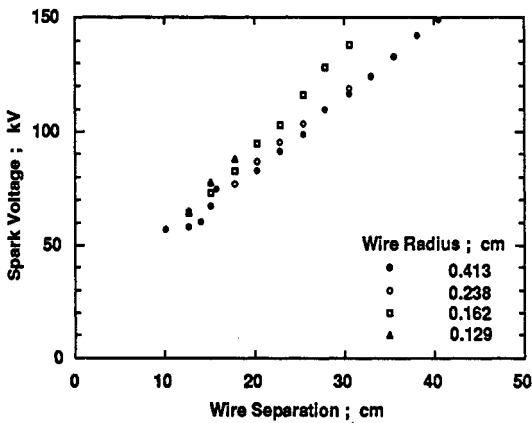


Fig.7 Spark Breakdown Voltage between Wires.

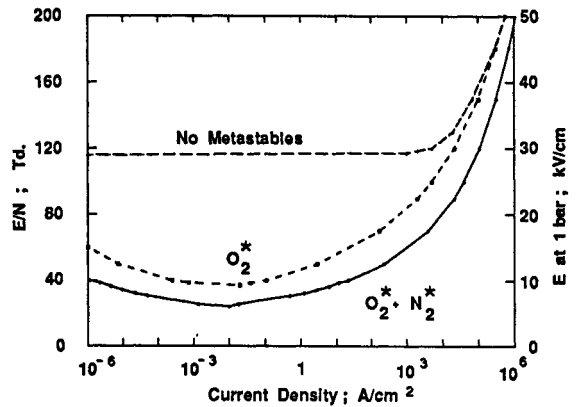
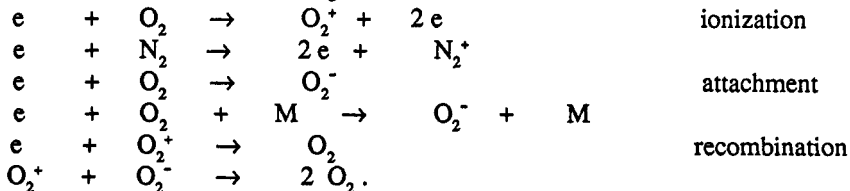


Fig.8 Calculated Effects of Metastables.

Fairly detailed analyses have been made of the chemistry of air and its products induced by either electric corona or electron beams. Matzing (16) has developed a chemical kinetic model with over 700 reactions, designed to study the removal of oxides of sulphur and nitrogen by irradiation with an electron beam. Using this chemical model, it is found that reactions with H and OH radicals from water vapor are of prime importance. Eliasson (17) and coworkers have developed a model with over 70 reactions to study ozone formation in corona discharges. Kossyi et al. have assembled kinetic equations with rate constants for over 250 reactions, involving only oxygen and nitrogen and their associated states and compounds (18).

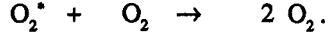
Of particular importance for properties of the corona discharge are reactions which affect the electron density. Equation (6) accounts for electron growth by ionization and electron removal by attachment and recombination. These reactions, including recombination between ions, are:



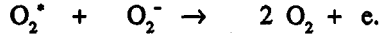
M represents a third body for three body attachment in oxygen.

However, there are other reactions that affect electron density, namely those in which metastables can induce the detachment of negative ions or additional ionization. To simplify analysis, and also to gain understanding of particular processes of plasma chemistry, we consider just two additional species, namely the $a^1\Delta_g$ metastable state of molecular oxygen, which we represent as O_2^* , and the a' metastable state of molecular nitrogen, which we represent as N_2^* . The $a^1\Delta_g$ state has a radiative lifetime of ~ 45 mins and a low quenching

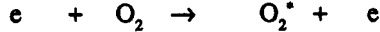
rate for collisions with oxygen, i.e.,



Of prime importance is that the metastables have the property of detaching O_2^- in the following reaction :



This reaction, whose rate constant is well established (19), reduces the effective attachment coefficient and thus modifies all analyses of corona discharges using the conventional attachment coefficient. The cross section for the rate of production of these metastables by the reaction



is also known so that the production rate of oxygen metastables is calculable for any gas mixture as a function of E/N . Production rates, m/M , calculated for air from ref.(3) are shown in Fig. 1.

CORONA THEORY INCLUDING PLASMA CHEMISTRY

To include the effect of oxygen metastables we would need to add an additional equation to our equations (6 - 8) for the density of metastables as a function of position and time. Similarly we would need to add a further equation to account for nitrogen metastables as it is claimed (20) that nitrogen a' metastable states produce new electrons by collisions with themselves according to the reaction



The production rate of these metastables is also calculable from known cross sections (21) and is also shown in Fig. 1. Furthermore, there is indirect evidence that metastable oxygen molecules produce ozone by collisions with themselves and a third body (22), and also that A state metastable nitrogen molecules (18) can detach negative ions. The problem rapidly becomes intractable. As the number of possible rate equations goes up with the square of the number of species, more and more rate constants of doubtful accuracy are needed.

To simplify the problem and to demonstrate the importance of plasma chemistry in corona, we solve equations (6 - 8) for the steady state for a uniform plasma and then compare the solution to that obtained with an additional equation for metastable oxygen molecules. Finally we add a further equation for a' state metastable nitrogen molecules. Equations (6), and (7), modified to include the effect of metastables, become

$$0 = n_e \alpha w_e - n_e \eta w_e - \gamma_R n_e n_+ + k_d \text{O}_2^* n_- \quad \text{and} \quad (10)$$

$$0 = n_e \alpha w_e - \gamma_R n_e n_+ - \gamma_R n_- n_+ \quad (11)$$

where k_d is the rate coefficient for detachment by metastables of $2.0 \times 10^{10} \text{ cm}^3 \text{ s}^{-1}$ and O_2^* represents the number density of metastable oxygen molecules. For equ. (8), we can simply write

$$n_- = n_+ - n_e, \quad (12)$$

as in the steady state positive and negative charge densities must be equal. Equating the production and destruction rates of oxygen metastables, we obtain an additional equation which is

$$0 = n_e m w_e - k_d \text{O}_2^* n_- - k_q \text{O}_2^* \text{O}_2; \quad (13)$$

m is the rate coefficient for the production of metastables from Fig. 1 and $k_q = 2.2 \times 10^{18} \text{ cm}^3 \text{ s}^{-1}$ is the two body rate constant for the quenching of metastables by oxygen (23).

We can now simplify the above four equations by eliminating n_- , n_+ and O_2^* to obtain a single equation in n_e and the transport coefficients and rate constants, i.e.,

$$\alpha - \eta - (\gamma_R \alpha n_e / w_e)^{1/2} + m - k_q m \text{O}_2 / [k_d (n_e \alpha w_e / \gamma_R)^{1/2} - k_d n_e + k_q \text{O}_2] = 0. \quad (14)$$

In equation (14), α , η and m are functions of E/N as shown in Fig.1. No arbitrary adjustment has been made to values of α/N at very low E/N as was done in ref. (3). From the solution of the Boltzmann equation, α/N at $E/N = 20 \text{ Td}$. is near zero, ie $1.7 \times 10^{-29} \text{ cm}^2$. The rate constants k_q and k_d are independent of E/N . The value of the recombination coefficient, γ_R , has been evaluated from $\gamma_R = \gamma_0 / T_e^{1/2}$, where the electron temperature, T_e , is evaluated from $k T_e / e = D / \mu$; k is Boltzmann's constant, D is the electron diffusion

coefficient and μ is the electron mobility. The value of γ_0 is taken as $2 \times 10^{-7} \text{ cm}^3 \text{ s}^{-1}$ from (24) and values of D/μ and w_e are taken as a function of E/N from (3). Thus for any given value of E/N , equ. (14) defines a value of electron density, n_e . The current density j , is defined by $j = n_e e w_e$. Thus equ. (14) defines a relationship between E/N and j for the existence of steady-state solutions for the glow state of the discharge. This relationship defines the volt-ampere characteristic of the discharge if its length and area are known.

In Fig. 8 are shown solutions of equ. (14) giving j as a function of E/N for air at atmospheric pressure. The curve marked "No Metastables" corresponds to the solution of equ. (14) with $m = 0$, i.e., for only the first three terms of equ. (14). Then, apart from the case of high current densities, the electric field must be such that ionization equals attachment, i.e. $E/N = 120 \text{ Td}$. Inclusion of the metastable terms in equ. (14) changes the solution significantly, as is seen from the curve marked O_2^* in Fig. 8. The curve marked $\text{O}_2^* + \text{N}_2^*$ in Fig. 8. is calculated with an additional term in equ (10) for the production of additional electrons from a' nitrogen atoms colliding with themselves. In this calculation, quenching processes are neglected and the additional electron production rate is calculated from the calculated rate of production of $\text{N}_2(a')$ molecules shown in Fig (1), where $\text{N}_2(a')$ is represented by N_2^* . The rate of production of N_2^* molecules is obtained from a solution of the Boltzmann equation for the electron distribution function using the cross sections for excitation of the a' state from ref. 21.

It is seen from Fig. 8 that the reactions of plasma chemistry including O_2^* and N_2^* change the properties of air so that the corona plasma can be sustained by a field of $\sim 6 \text{ kV/cm}$ at atmospheric pressure instead of the field of 30 kV/cm for ordinary air. It is seen from Figs. 4 and 6 that space charge effects tend to make the initial highly non-uniform electrostatic field uniform across any gap. If the applied voltage is sufficient to provide such a field across any discharge gap, an arc is likely to form and there would be spark breakdown. The curve of Fig 8 including O_2^* and N_2^* reactions has a minimum field of $\sim 6 \text{ kV/cm}$. It is considered likely that inclusion of further processes of plasma chemistry would explain the results of Fig. 7 which shows that the spark breakdown occurs for a field of $\sim 4 \text{ kV/cm}$.

REFERENCES

1. S.Masuda and H.Nakao, *IEEE Trans. on Industry Applications*, **26**, 374 (1990).
2. F.W.Peek Jr., *Dielectric Phenomena in High Voltage Engineering*, p. 66, McGraw-Hill, New York (1929).
3. J.J.Lowke, *J. Phys D: Appl. Phys.* **25**, 202 (1992).
4. F.Llewellyn-Jones, *Ionization and Breakdown in Gases*, Methuen, London (1966).
5. J.D.Cobine, *Gaseous Conductors*, Dover, New York (1958).
6. J.S.Townsend, *Electricity in Gases*, Oxford, Clarendon (1915).
7. M.Goldman and A.Goldman, *Gaseous Electronics*, Vol 1. p. 219, Academic, London (1978).
8. L.B.Loeb, *Electrical Coronas*, University of California Press, Berkeley (1965).
9. R.S.Sigmond, *Corona Discharges*, Ch. 4 of *Electrical Breakdown in Gases*, edited by J.Meek and J.D.Craggs, (1978).
10. G.W.Trichel, *Phys. Rev.*, **54**, 1078 (1938).
11. R.Morrow, *Phys. Rev. A*, **32**, 1799 (1985).
12. R.Morrow, *IEEE Trans. Elect. Insul.* **26**, 398 (1991).
13. R.Morrow, *IEEE Trans. Plasma Sci.* **19**, 86 (1991).
14. A.J.Davies, C.J.Evans and F.Llewellyn-Jones, *Proc Roy.Soc. A*, **281**, 164 (1964).
15. R.Morrow and L.E.Cram, *J. Comp. Phys.* **57**, 129 (1985).
16. H.Matzing, *Advances in Chemical Physics*, **80**, 315 (1991).
17. B.Eliasson, M. Hirth and U.Kogelschatz, *ISPC*, Eindhoven, p. 339 (1985) and Tokyo, p. 736 (1987).
18. I.A.Kossyi, A.Yu Kostinsky, A.A.Matveyev and V.P.Silakov, *Plasma Sources Science Tech.* **1**, 207 (1992).
19. F.C.Fehsenfeld, D.L.Albritton, J.A.Burt and H.I.Schiff, *Can. J. Chem.*, **47**, 1793 (1969)
20. H.Brunet and J.Rocca-Serra, *J. Appl. Phys.* **57**, 1574 (1985).
21. A.V.Phelps and L.C.Pitchford, *Phys. Rev. A*, **31**, 2932 (1985).
22. G.Fournier, R.Lucas and D.Pigache, *Bull. Am. Phys. Soc.* **23**, 146 (1978).
23. F.D.Findlay and D.R.Snelling, *J. Chem. Phys.* **55**, 545 (1971).
24. R.Johnsen, *Int.J.Mass Spectrom. Ion Phys.* **81**, 67 (1987).